

Characterisation of Electroless Deposited Cobalt by Hard and Soft X-ray Photoemission Spectroscopy

A. Brady-Boyd¹, R. O'Connor¹, S. Armini², V. Selvaraju¹, G. Hughes¹ and J. Bogan¹

¹School of Physical Sciences, Dublin City University, Glasnevin, Dublin 9, Ireland email: anita.brady32@mail.dcu.ie

²IMEC, Kapeldreef 75, B-3001 Heverlee, Leuven, Belgium

Abstract— Electroless deposited (ELD) cobalt with palladium as a catalyst, and an underlying self-assembled monolayer (SAM) was investigated for potential use in advanced complementary metal oxide semiconductor (CMOS) applications using both hard (HAXPES) and soft (XPS) x-ray photoelectron spectroscopy. HAXPES spectra established the uniformity of the deposited Co film and the nature of the buried Co-Si interface ~20nm below the surface. The Pd is seen to diffuse through the Co following thermal annealing. While the deposited Co film is predominantly metallic, Co-silicide forms at the Co-Si interface upon deposition and decomposes with thermal anneal up to 500 °C.

I. INTRODUCTION

With the continued aggressive scaling toward smaller feature sizes, the need has arisen for alternative materials to copper to act as the interconnect metal. Various materials such as metal silicides [1, 2], graphene [3] and Co [4, 5] are currently being investigated to replace Cu. With such small dimensions it can be difficult for deposition techniques such as chemical and physical vapour deposition (CVD, PVD) to achieve seamless fill of high aspect ratio trenches. Traditional bottom-up electrodeposition methods require a conductive seed layer whose continuity is a challenge in high aspect ratio and small pitch structures. An electroless deposition (ELD) approach can provide viable solutions for these problems. An ELD process is attractive due to the fact it can be used to deposit on metals and insulators upon catalyst placement, it can achieve very uniform thin films, and it is a relatively low-cost process. ELD cobalt is a strong candidate to fully replace copper as the via prefill or interconnect Jiang *et al* [4] and Van der Veen *et al* [5] have shown that using cobalt as the via metal, it can outperform copper with feature sizes below 28 nm and 15 nm respectively, in terms of resistance and electromigration resistance. In this method there is no barrier required for dense low-k dielectrics, so the cobalt is free to take up the full area of the via. In the newest technology node In the newest technology node Co has replaced Cu in the first three metal lines [6]. SAMs have also been demonstrated as a valuable adhesion promoter, potential pore sealant for low-k dielectrics, and as a blocker for use in selective area atomic layer deposition (ALD) [7, 8].

II. EXPERIMENTAL DETAILS AND METHOD

Native silicon dioxide on Si (100) substrates were cleaned by 15-minute exposure to UV-ozone treatment in a Jelight UVO Cleaner. Subsequently, SAMs derived from (3-trimethoxysilylpropyl) diethylenetriamine (DETA) precursor were deposited via vapour phase deposition on the UVO cleaned substrates. SAM films were deposited using 100 μ L of the precursor at a temperature of 140°C for 1 hr with a chamber pressure of \approx 10 mbar. The substrates were then immersed in a PdCl₂ acidic solution, with a pH of 2, for 2 minutes and then rinsed for 2 minutes with deionized (DI) water. Co was deposited by ELD to a thickness of 20 nm from a solution of CoSO₄, NH₄Cl and water with a dimethyl ammonium borane (DMAB) reducing agent. Following Co deposition, the samples were annealed in a forming gas atmosphere at 420°C for 15 minutes.

HAXPES and XPS measurements were performed at Diamond Light Source, UK. Due to the high photon energy employed by HAXPES, buried interfaces up to ~20nm deep are accessible compared to ~8nm in conventional XPS. In this facility one can illuminate a precise location on the sample under consideration using both soft and hard x-rays simultaneously. This gives the unique advantage of concurrently recording surface and bulk properties during each experimental step. The soft x-ray incident photon energy was 1.2 keV, while the hard x-ray incident photon energy was 5.9 keV. A VG Scienta EW4000 HAXPES energy analyser was used to record the spectra. The sample was placed in the ultra-high vacuum chamber at a base pressure of $\sim 5 \times 10^{-10}$ mbar. The sample received three anneals; 300°C, 400°C and 500°C in-vacuo and photoemission spectra were acquired after each anneal. All spectra are shifted to the C 1s at a binding energy position of 284.8eV.

III. RESULTS AND DISCUSSION

A. Characterisation of ELD Co Films

In this study DETA is employed as an adhesion promoter for the Pd. The Pd adheres to the amino terminal group of the DETA and forms a seed layer (~1nm) for the ELD Co. Survey spectra taken in the hard x-ray (Fig. 1(a)) regime are dominated by the ELD Co signal while the soft x-ray (Fig. 1(b)) regime is dominated by the oxygen signal from surface oxide. One important point to note is that the Si 1s, at a binding energy of ~1839eV, is visible in the HAXPES scans.

This indicates that the entirety of the Co film (~20nm) is accessible as the only source of Si is the underlying substrate. From the ELD deposition, nitrogen, carbon, and boron have been incorporated into the film with the carbon and nitrogen concentrations decreasing with thermal annealing. This is observed in both hard and soft regimes. The Pd does not become evident until after the 400°C anneal. The nitrogen and palladium are not easily observed in the survey spectra but are accessible in narrow energy window scans. The soft X-ray spectra show a large increase in intensity in both the B 1s and O 1s following thermal annealing.

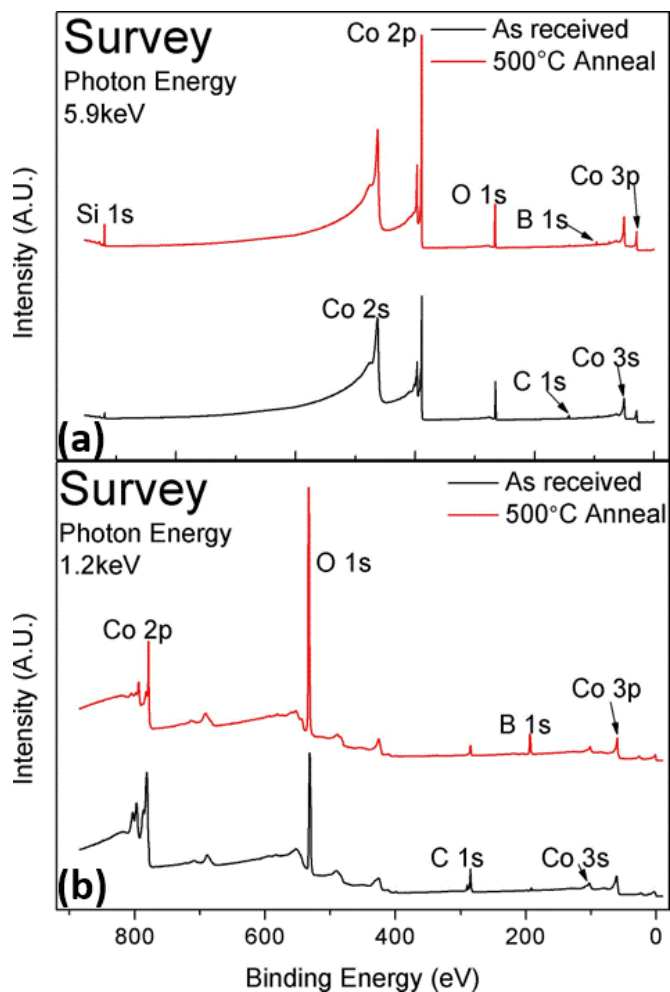


Fig. 1(a) Hard and (b) soft X-ray survey scans showing the first and last experiment steps. All peaks are labeled except for the N 1s and Pd 3d which are not easily seen in the survey spectra.

Fig.2 shows the Pd 2p which a literature review suggests, is the first-time this peak has been investigated with HAXPES. The Pd does not become evident until after the 400°C anneal has been performed. One possible reason for this is that the Pd is diffusing through the Co film. The peak appears to be in a metallic state with the $2p_{3/2}$ at binding energy of 3174.3eV and the $2p_{1/2}$ at a binding energy of 3331.3eV and a possible oxide shoulder on the higher binding energy side of both peaks. This was determined by analysis of the Pd 3d (not shown) which has a binding energy of 335.4eV and is therefore in the correct position for Pd metal.

Fig.3 shows the Co 2p spectrum recorded with both hard and soft x-rays. From the HAXPES spectrum in Fig.3(a) the as-received sample shows a small surface oxide, which is present on the higher binding energy (HBE) side of the metallic component peak. This peak intensity is decreased by the sequence of anneals and by the 500°C anneal the oxide is

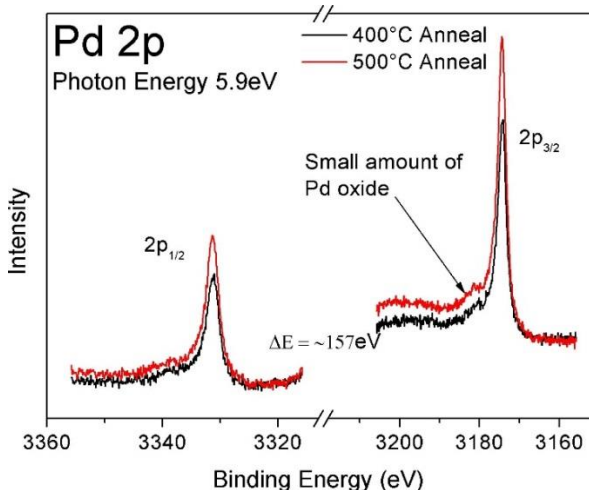


Fig. 2 The Pd 2p spectrum showing a metallic profile with a slight oxide on the HBE side of the peak.

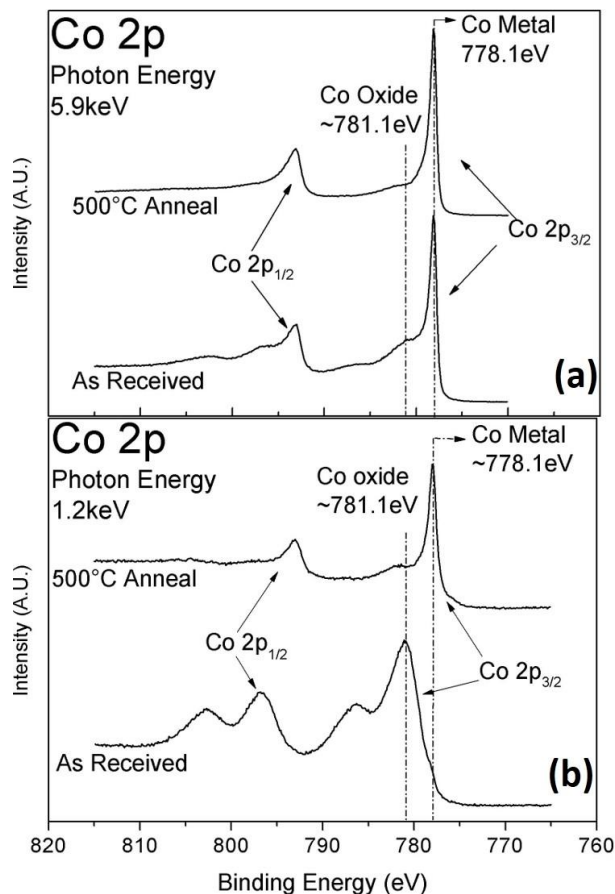


Fig. 3 The Co 2p in the (a) hard X-rays shows a mostly metallic peak with some oxide in the HBE side. The (b) soft X-ray scans reveal that this oxide is surface localized. Both spectra show how this oxide is removed with thermal anneal.

almost completely removed. The XPS spectra in Fig.3(b) confirm that the oxide is surface localized. The data suggests that the top ~5nm is primarily Co-oxide. There is however, a small metallic shoulder on the lower binding energy (LBE) side of the oxide peak. This can be seen to grow with each thermal anneal while the oxide component decreases until finally after the 500 °C anneal the surface oxide has been almost removed. These spectra demonstrate that the ELD process has deposited a high quality metallic film in which the residual surface oxide is easily reduced by thermal annealing.

To ascertain if there was any evidence of the DETA SAM, the high energy spectra of the C 1s and N 1s (Fig. 4) were examined. The N 1s has just one broad peak with two component peaks. These peaks have been attributed to C-N-O bonds at 399.35 eV and the other is attributed to boron nitride (BN) at 398.1 eV. The reducing agent used during the ELD process is the source of boron. The signal to noise ratio is poorer for the nitrogen than the other spectra due to small quantity of nitrogen in the film. With subsequent anneals this signal to noise ratio deteriorates, as these nitrogen species decompose and the corresponding peak intensity decreases. In soft X-rays spectra (not shown) there is a N 1s peak present. If the only source of N is the DETA SAM, then there should be no visible N 1s peak in these spectra as the soft X-rays are surface sensitive (~8nm). This would imply that N has been incorporated into film. However, this makes identifying the DETA SAM extremely difficult.

Looking at the C 1s initially there are two main peaks with several component peaks, visible in the spectra. A peak at LBE which is attributed to C-C bonds at 284.8eV, C-O / C-N-O bonds at ~286eV, C=O bonds at ~288.4eV and a peak at HBE which has been attributed to cobalt carbonate at 289.8eV. Following the 300°C anneal the carbonate peak intensity is greatly reduced and by the 500°C anneal it has been fully decomposed. The C=O component peak is also removed by the thermal anneals. The main component peak remains quite strong throughout the experiment and suggests that the C has become incorporated into the film during the ELD process. This again makes identifying the C signal from the DETA SAM very difficult.

Fig. 5 displays the deconvoluted hard X-ray O 1s and B 1s spectra. The as-received spectra show the B has formed Co-boride and BN while the Co oxide and carbonate dominated the O 1s. Also, present in the O 1s is a small boron oxide peak which grows upon anneal. This can also be seen in the B 1s following the 300°C anneal. The oxygen released from the decomposition of the Co oxide and carbonate is not desorbed from the surface but instead forms a bond with the B to form a boron oxide. As the B oxidizes further both spectra can be seen to shift to a higher binding energy. By the 500°C anneal the boron has become fully oxidised by forming B₂O₃. The corresponding component peaks in both the B 1s (193.3 eV) and O 1s (532.9eV) are now in the correct binding energy position for B₂O₃ [9, 10].

B. The Si-Co Interface

In order to understand the interactions between the Co overlayer and the silicon substrate, the Si 1s peak was studied in detail and the deconvoluted spectra is presented in Fig. 6. Initial data from the as-received sample reveals the Si to

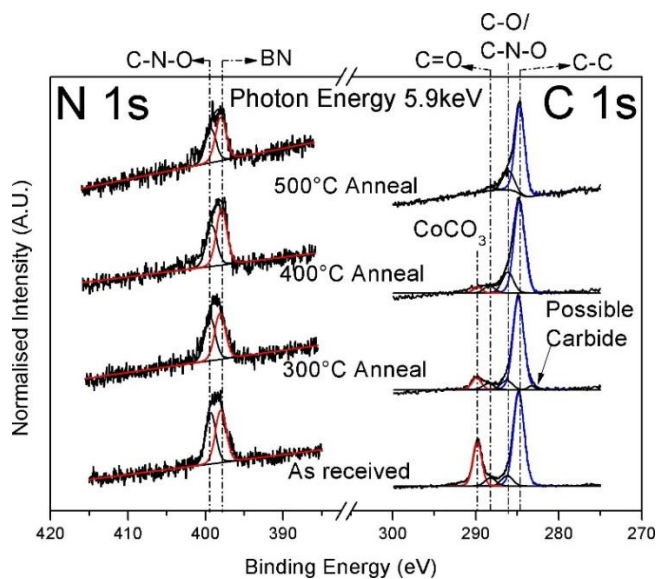


Fig.4 The normalised N 1s and C 1s, show a deterioration in the signal to noise for the N 1s and the decomposition of the C 1s with increasing anneal temperature

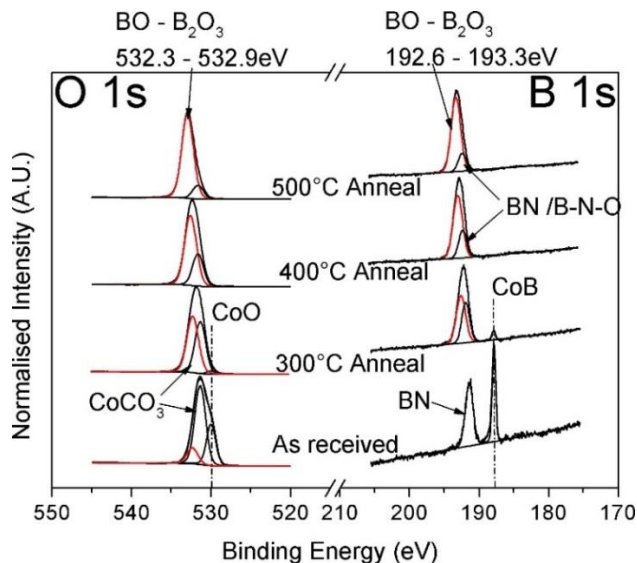


Fig. 5 The deconvoluted O 1s and B 1s hard X-ray spectra showing the reduction of the CoO and CoCO₃ and the oxidation of the B 1s.

comprise of several different components which have been assigned to the bulk Si at 1839.1 eV, two Co silicide phases, one at 1839.5eV and the other at 1838.7eV, SiO₂ at 1843.7eV and sub oxide states on the HBE side of the bulk peak. The silicide phase on the HBE side has been attributed to CoSi [9, 10] while the silicide on the LBE side has been attributed to Co₂Si [11, 12]. There is also a “pre-peak” observed on the LBE side. This “pre-peak” has previously been observed in a Si 1s iron silicide spectra [15]. Following the 300°C anneal

the Co_2Si phase grows significantly while the bulk Si component peak reduces as it is consumed to form more silicide. The 400°C anneal sees the breakdown of this phase as the bulk Si signal increases.

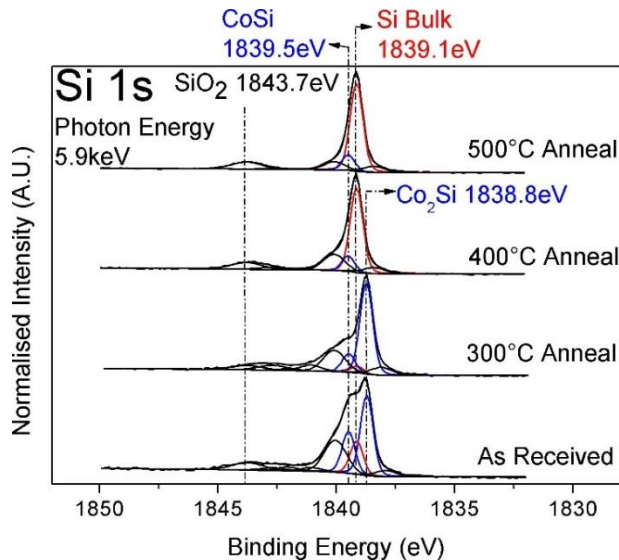


Fig.5 Peak fitted Si 1s Spectra showing two silicide phases which with thermal anneal decompose.

The Si^{2+} and the Si^{3+} sub oxides have almost completely decomposed and released enough oxygen to breakdown this Co rich phase. The CoSi phase being more stable, remains. By the 500°C the bulk Si, CoSi and SiO_2 peaks have become stable and have not changed appreciably since the last anneal. The Si^{1+} is still quite large but it is expected with a higher annealing temperature that this oxide phase would decompose.

IV. CONCLUSION

From this study it can be concluded that SAMs have been successful in trapping the Pd which in turn was successful in promoting the reaction for the electroless deposition. High energy spectra show that the Co film is a superior quality metallic film with a small amount of surface oxide present which can be eliminated by thermal annealing. The quality of the film is of the utmost importance for devices as any oxide can decrease the conductivity. It is clear that boron has become incorporated into the film and bonds with the released oxygen to form B_2O_3 . The carbon and nitrogen introduced from the deposition, reduce with each thermal anneal. It cannot be confirmed if the DETA SAM has survived the ELD process or if it has been etched away. It has been shown that the ELD process forms two cobalt silicide phases at the Si-Co interface which are unstable at high temperatures.

ACKNOWLEDGMENT

The authors would like to gratefully acknowledge financial support from the SFI PI Programme under Grant No. 13/1A/1955. The authors also gratefully acknowledge Diamond Light Source for time on beamline i09 under proposal SI19698-1. The research leading to this result has been supported by the project CALIPSOplus under the Grant Agreement 730872 from the EU Framework Programme for Research and Innovation HORIZON 2020. This work was carried out within the IMEC Industrial Affiliation Programme on Advanced Interconnects (IIAP).

REFERENCES

- [1] Z. W. Zhu, X. D. Gao, Z. Bin Zhang, Y. H. Piao, C. Hu, D. W. Zhang, and D. P. Wu, "Formations and morphological stabilities of ultrathin CoSi 2 films," *Chinese Phys. B*, vol. 21, no. 8, 2012.
- [2] M. Bhaskaran, S. Sriram, T. S. Perova, V. Ermakov, G. J. Thorogood, K. T. Short, and A. S. Holland, "In situ micro-Raman analysis and X-ray diffraction of nickel silicide thin films on silicon," *Micron*, vol. 40, no. 1, pp. 89–93, 2009.
- [3] I. Asselberghs, M. Politou, B. Soree, S. Sayan, D. Lin, P. Pashaei, C. Huyghebaert, P. Raghavan, I. Radu, and Z. Tokei, "Graphene wires as alternative interconnects," in *2015 IEEE International Interconnect Technology Conference and 2015 IEEE Materials for Advanced Metallization Conference (IITC/MAM)*, 2015, pp. 317–320.
- [4] Yu Jiang, P. Nalla, Y. Matsushita, G. Harm, Jingyan Wang, A. Kolics, L. Zhao, T. Mountsier, P. Besser, and Hui-Jung Wu, "Development of electroless Co via-prefill to enable advanced BEOL metallization and via resistance reduction," in *2016 IEEE International Interconnect Technology Conference / Advanced Metallization Conference (IITC/AMC)*, 2016, pp. 111–113.
- [5] M. H. Van Der Veen, K. Vandersmissen, D. Dictus, S. Demuyneck, R. Liu, X. Bin, P. Nalla, A. Lesniewska, L. Hall, K. Croes, L. Zhao, J. Bömmels, A. Kolics, and Z. Tökei, "Cobalt bottom-up contact and via prefill enabling advanced logic and DRAM technologies," in *2015 IEEE International Interconnect Technology Conference and 2015 IEEE Materials for Advanced Metallization Conference, IITC/MAM 2015*, 2015, no. v, pp. 25–27.
- [6] C. Auth, A. Aliyarukunju, M. Asoro, D. Bergstrom, V. Bhagwat, J. Birdsall, N. Bisnik, M. Buehler, V. Chikarmane, G. Ding, Q. Fu, H. Gomez, W. Han, D. Hanken, M. Haran, M. Hattendorf, R. Heussner, H. Hiramatsu, B. Ho, S. Jaloviar, I. Jin, S. Joshi, S. Kirby, S. Kosaraju, H. Kothari, G. Leatherman, K. Lee, J. Leib, A. Madhavan, K. Marla, H. Meyer, T. Mule, C. Parker, S. Parthasarathy, C. Pelto, L. Pipes, I. Post, M. Prince, A. Rahman, S. Rajamani, A. Saha, J. D. Santos, M. Sharma, V. Sharma, J. Shin, P. Sinha, P. Smith, M. Sprinkle, A. St. Amour, C. Staus, R. Suri, D. Towner, A. Tripathi, A. Tura, C. Ward, and A. Yeoh, "A 10nm high performance and low-power CMOS technology featuring 3rd generation FinFET transistors, Self-Aligned Quad Patterning, contact over active gate and cobalt local interconnects," *2017 IEEE Int. Electron Devices Meet.*, p. 29.1.1-29.1.4, 2017.
- [7] A. Brady-Boyd, R. O'Connor, S. Armini, V. Selvaraju, G. Hughes, and J. Bogan, "On the use of (3-trimethoxysilylpropyl)diethylenetriamine self-assembled monolayers as seed layers for the growth of Mn based copper diffusion barrier layers," *Appl. Surf. Sci.*, vol. 427, pp. 260–266, 2018.
- [8] F. S. Minaye Hashemi, B. R. Birchansky, and S. F. Bent, "Selective Deposition of Dielectrics: Limits and Advantages of Alkanethiol Blocking Agents on Metal-Dielectric Patterns," *ACS Appl. Mater. Interfaces*, vol. 8, no. 48, pp. 33264–33272, 2016.
- [9] B. J. Matsoso, K. Ranganathan, B. K. Mutuma, T. Leretholi, G. Jones, and N. J. Coville, "Synthesis and characterization of boron carbon oxynitride films with tunable composition using methane, boric acid and ammonia," *New J. Chem.*, vol. 41, no. 17, pp. 9497–9504, 2017.
- [10] Z. Pan, Y. Yang, J. Huang, B. Ren, H. Yu, R. Xu, H. Ji, L. Wang, and L. Wang, "Study on the preparation of boron-rich film by magnetron sputtering in oxygen atmosphere," *Appl. Surf. Sci.*, vol. 388, pp. 392–395, 2016.
- [11] J. S. Pan, R. S. Liu, Z. Zhang, S. W. Poon, W. J. Ong, and E. S. Tok, "Co growth on $\text{Si}(0\ 0\ 1)$ and $\text{Si}(1\ 1\ 1)$ surfaces: Interfacial interaction and growth dynamics," *Surf. Sci.*, vol. 600, no. 6, pp. 1308–1318, 2006.
- [12] I. Y. Hwang, J. H. Kim, S. K. Oh, H. J. Kang, and Y. S. Lee, "Ultrathin cobalt silicide film formation on $\text{Si}(100)$," *Surf. Interface Anal.*, vol. 35, no. 2, pp. 184–187, 2003.
- [13] M. V. Gomoyunova, G. S. Grebenyuk, and I. I. Pronin, "Binding energies of Si 2p and Co 3p electrons in cobalt silicides," *Tech. Phys. Lett.*, vol. 37, no. 12, pp. 1124–1126, 2011.
- [14] C. Van Bockstael, K. De Keyser, J. Demeulemeester, A. Vantomme, R. L. Van Meirhaeghe, C. Detavernier, J. L. Jordan-Sweet, and C. Lavoie, "In situ study of the formation of silicide phases in amorphous Co-Si mixed layers," *Microelectron. Eng.*, vol. 87, no. 3, pp. 282–285, 2010.
- [15] L. Badía-Romano, J. Rubín, F. Bartolomé, C. Magén, J. Bartolomé, S. N. Varnakov, S. G. Ovchinnikov, J. Rubio-Zuazo, and G. R. Castro, "Morphology of the asymmetric iron-silicon interfaces," *J. Alloys Compd.*, vol. 627, pp. 136–145, 2015.

